Electronic Supplementary Material (ESI) for Dalton Transactions

Supporting Information

Ionothermal synthesis of two oxalate-bridged lanthanide(III) chains with slow magnetization relaxation by using deep eutectic solvent

Yan-Meng, Jun-Liang Liu, Ze-Min Zhang, Wei-Quan Lin, Zhuo-Jia Lin and Ming-Liang Tong*

MOE Key Laboratory of Bioinorganic and Synthetic Chemistry / State Key Laboratory of Optoelectronic Materials and Technologies, School of Chemistry and Chemical Engineering, Sun Yat-Sen University, Guangzhou 510275, China. E-mail: tongml@mail.sysu.edu.cn

Experimental details

General Remarks: The reagents for the synthesis were commercially available and used as purchased without further purification. The C, H and N microanalyses were carried out with an Elementar Vario-EL CHNS elemental analyzer. The FT-IR spectra were recorded from KBr pellets in the range 4000-400 cm^{-1} on a Bio-Rad FTS-7 spectrometer. Powder X-ray diffraction measurements have been obtained on Bruker D8 Advance Diffratometer (Cu-Kα, λ = 1.54056 Å) by scanning over the range of 5-50° with a step of 0.12 °/s at 293 K. Simulated powder XRD patterns were calculated with Mercury. Magnetic susceptibility Data was measured by a Quantum Design MPMS-XL7 SQUID. Data were corrected for the diamagnetic contribution calculated from Pascal constants.

Synthesis of 1: A mixture of $DyCl_3 \cdot 6H_2O$ (0.263 g, 0.7 mmol), Choline Chloride (0.267 g, 2 mmol) and Oxalic acid dehydrate (0.265g, 2 mmol) were sealed in a 20 mL Teflon-lined autoclave and heated at 120 °C for 3 days. Colorless transparent needle-shaped crystals were washed by methanol, dried in air and recovered with 57% (based on Dy). IR (KBr, cm^{-1}): 3448(br, vs), 3390(br), 3328(br), 3170(br, vs), 2246(w), 2165(w), 2069(w), 1643(vs), 1465, 1390(vs), 1311(vs), 1267(s), 1164(m), 1116(m), 1085(m), 1039(w), 966(w), 921, 788(s), 671(s), 632(m), 553(m), 512(w), 460(w). Elemental analyses (calc: found) for **1**: C 16.89 : 16.95, H 4.46 : 4.34, N 2.81 : 2.78.

Synthesis of 2: The procedure was the same as that employed for **1**, except that $ErCl_3 \cdot 6H_2O$ (0.267 g, 0.7 mmol) was employed as lanthanide salts. The pink needle-shaped crystals were obtained (yield 51 % based on Er). IR (KBr, cm^{-1}): 3450(br, vs), 3386(br), 3318(br), 3167(br, vs), 2290, 2188, 2081, 1910, 1625(vs), 1469, 1390(vs), 1317(vs), 1270(s), 1159(m), 1118(m), 1089(m), 1039(w), 971(w), 946, 916, 788(s), 671(s), 619(m), 551(m), 512(w), 468(w). Elemental analyses (calc: found) for **2**: C 16.73 : 16.73, H 4.41 : 4.31, N 2.79 : 2.49.

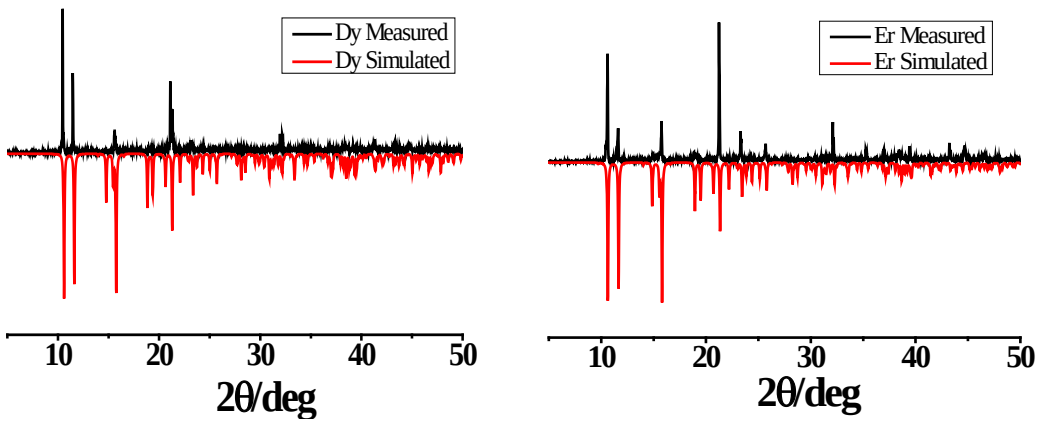

Fig. S1 Powder X-ray diffraction patterns of compounds **1** (*left*) and **2** (*right*).

Crystal data for **1**: $C_7H_{22}DyNO_9Cl_2$, M = 497.66, Monoclinic, space group $P2_1/n$, a = 9.118(2), b = 15.223(4), c = 12.154(3) Å, α = 90°, β = 109.432(5)°, γ = 90°, V = 1590.9(7) Å^3, T = 150(2) K, Z = 4, ρ_c = 2.078 g cm^{-3}, F(000) = 972, 3395 reflections collected, 2560 reflections used (R_{int} = 0.0423), R_1 = 0.0585 ($I > 2\sigma(I)$), wR_2 = 0.1117 (all data). For **2**: $C_7H_{22}ErNO_9Cl_2$, M = 502.42, Monoclinic, space group $P2_1/n$, a = 9.0957(2), b = 15.1667(3), c = 12.0825(3) Å, α = 90°, β = 109.627(2)°, γ = 90°, V = 1569.96(6) Å^3, T = 150(2) K, Z = 4, ρ_c = 2.126 g cm^{-3}, F(000) = 980, 2355 reflections collected, 2141 reflections used(R_{int} = 0.0284), R_1 = 0.0396 ($I > 2\sigma(I)$), wR_2 = 0.0769 (all data). Diffraction data for **1** were recorded on a Rigaku R-AXIS SPIDER Image Plate diffractometer with graphite-monochromated Mo-Kα (λ = 0.71073 Å) radiation at 150(2) K. Diffraction data for **2** were carried out with the Oxford-Diffraction Xcalibur CCD diffractometer using graphite-monochromated Cu-Kα radiation (λ = 1.54178 Å) at 150(2) K.

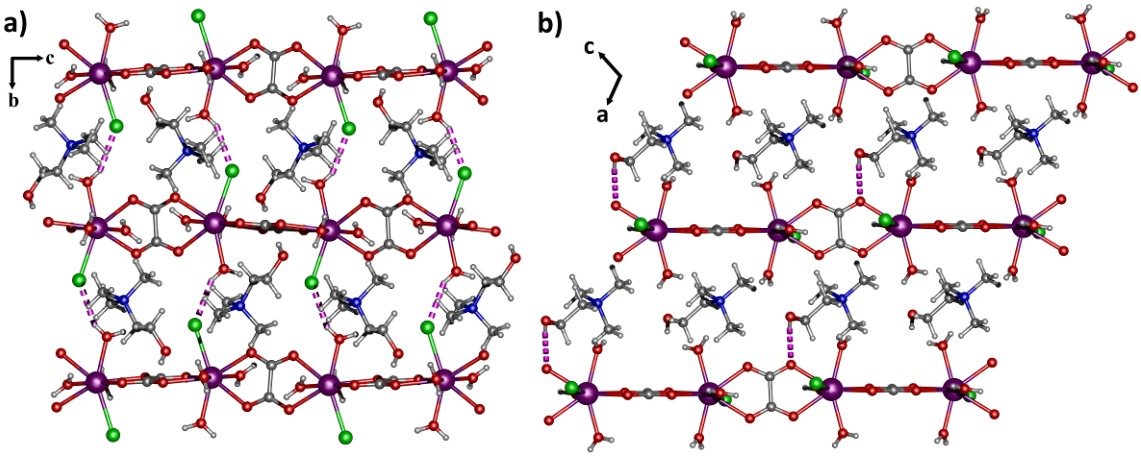

Fig. S2 Ball and stick plots from viewpoints along the *a* axis (**a**) and the *b* axis (**b**). Hydrogen bonds are represented by pink dashed line.

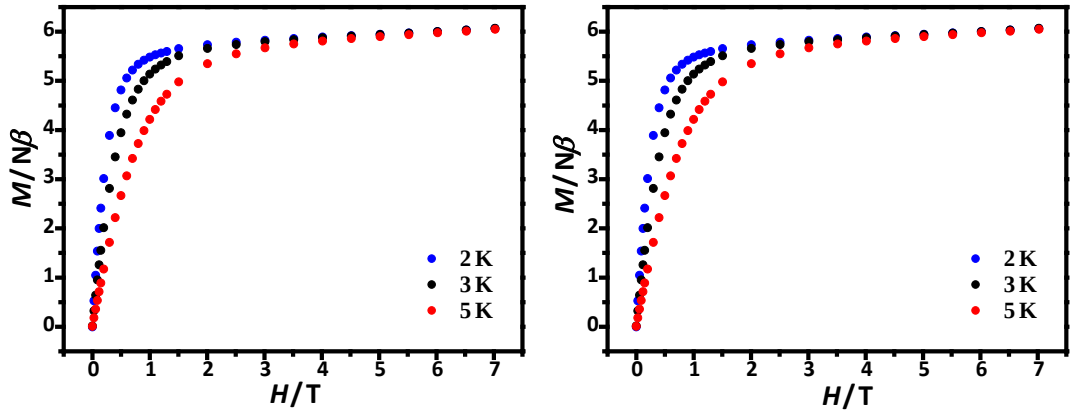

Fig. S3 Field-dependence of the magnetization at the indicated temperatures for **1** (*left*) and **2** (*right*).

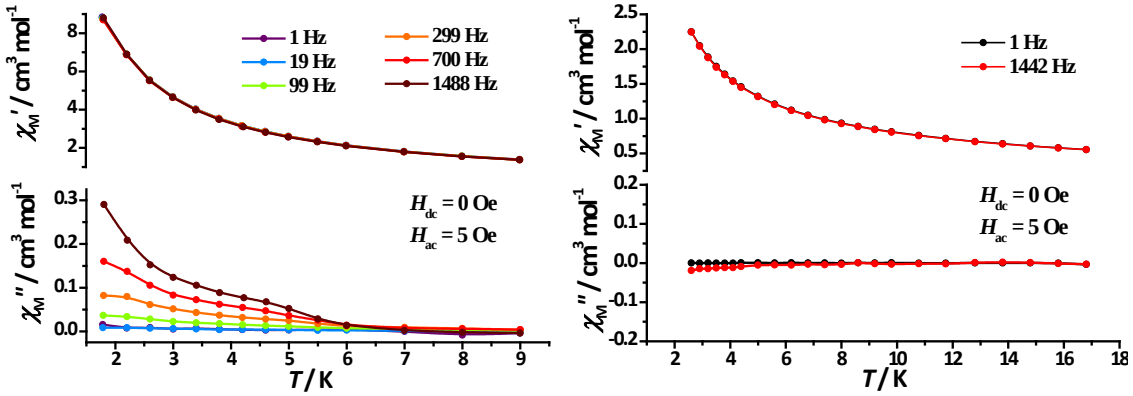

Fig. S4 Temperature-dependence of in-phase (χ_M') and out-of-phase (χ_M'') ac susceptibility signals (H_{dc} = 0 Oe, H_{ac} = 5 Oe) at the indicated frequencies for **1** (left) and **2** (right).

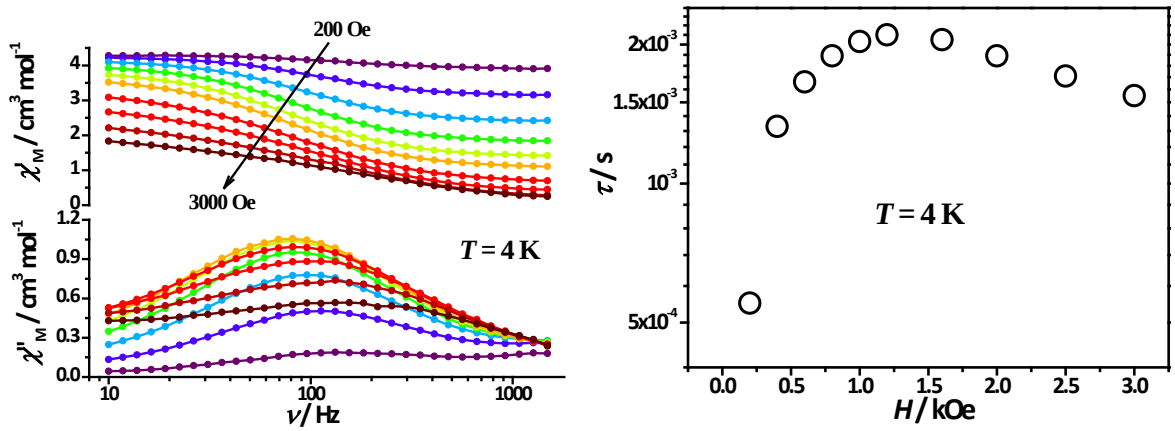

Fig. S5 *Left*: Plot of ac susceptibility *vs* frequency (ν) in the applied fields of 200-3000 Oe at 4 K for **1**; *Right*: dc field dependence of the relaxation time at 4 K.

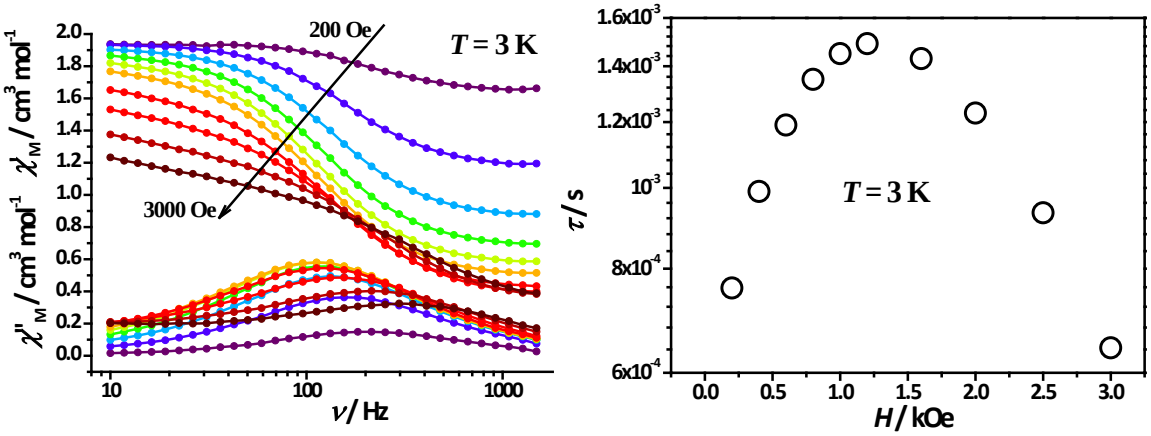

Fig. S6 *Left*: Plot of ac susceptibility *vs* frequency (ν) in the applied fields of 200-3000 Oe at 3 K for **2**; *Right*: dc field dependence of the relaxation time at 3 K.

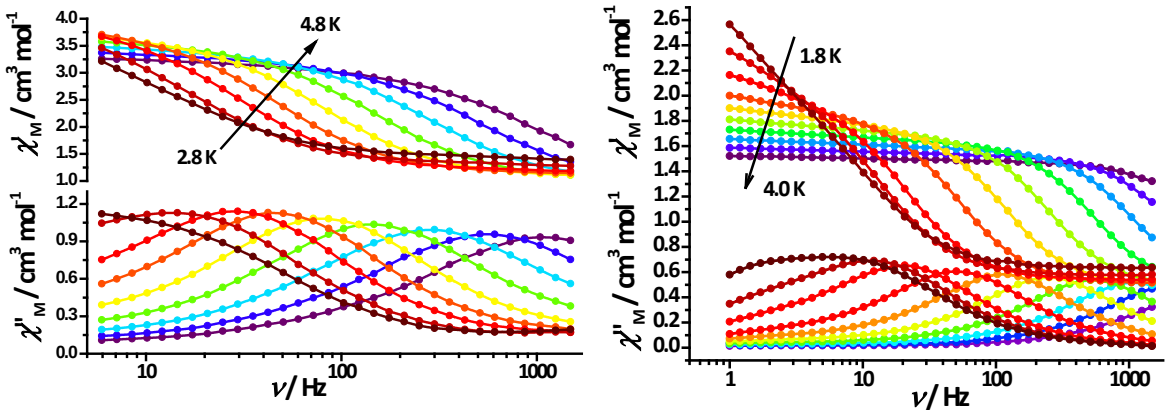

Fig. S7 Frequency-dependence of ac susceptibility signals (H_{dc} = 1200 Oe, H_{ac} = 5 Oe) in the temperature range of 2.8-4.8 K for **1** (right) and 1.8-4.0 K for **2** (left).